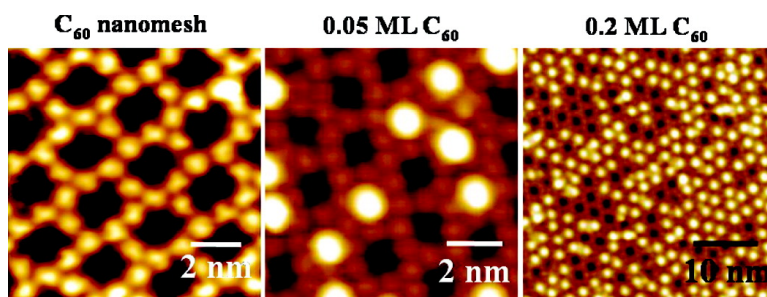


## Preferential Trapping of C in Nanomesh Voids

Hong Liang Zhang, Wei Chen, Han Huang, Lan Chen, and Andrew Thye Shen Wee

*J. Am. Chem. Soc.*, **2008**, 130 (9), 2720-2721 • DOI: 10.1021/ja710009q

Downloaded from <http://pubs.acs.org> on February 8, 2009



### More About This Article

Additional resources and features associated with this article are available within the HTML version:

- Supporting Information
- Links to the 4 articles that cite this article, as of the time of this article download
- Access to high resolution figures
- Links to articles and content related to this article
- Copyright permission to reproduce figures and/or text from this article

[View the Full Text HTML](#)



## Preferential Trapping of C<sub>60</sub> in Nanomesh Voids

Hong Liang Zhang,<sup>†</sup> Wei Chen,<sup>\*†</sup> Han Huang,<sup>†</sup> Lan Chen,<sup>‡</sup> and Andrew Thye Shen Wee<sup>\*†</sup>  
Department of Physics and Nanoscience and Nanotechnology Initiative, National University of Singapore,  
2 Science Drive 3, 117542, Singapore

Received November 5, 2007; E-mail: phycw@nus.edu.sg; phyweets@nus.edu.sg

The controlled fabrication of ordered two-dimensional (2D) molecular nanostructure arrays represents a major challenge for the realization of molecule-based miniature devices in the fields of molecular electronics,<sup>1</sup> quantum computers,<sup>2</sup> and biosensors.<sup>3</sup> Surface nanotemplate-assisted molecular assembly offers a promising approach toward the “bottom-up” construction of addressable functional molecular architectures through inherent processes of molecular adsorption, surface diffusion, and nucleation.<sup>4</sup> An effective surface nanotemplate usually features prepatterned and well-ordered preferential adsorption sites that can selectively accommodate guest adsorbates (molecules or atoms). In the past few years, intensive efforts have been devoted to the fabrication of various surface nanotemplates, as well as the detailed investigation of the molecular assembly processes on these nanotemplates.<sup>4–13</sup> In particular, recent advances in molecular self-assembly have led to a new type of nanotemplates, referred to as 2D supramolecular porous networks, stabilized by directional noncovalent intermolecular interactions.<sup>8–13</sup> These self-assembled networks have been demonstrated to act as efficient templates to selectively accommodate guest molecules at pore sites, thereby leading to the formation of a variety of striking well-ordered molecular nanostructure arrays. Elegant examples include C<sub>60</sub> honeycomb arrays on a hydrogen-bonded supramolecular network,<sup>8</sup> C<sub>60</sub> molecules on a 2D porphyrin-based porous network,<sup>9</sup> C<sub>60</sub> molecules steered by metal–organic coordination porous networks,<sup>13</sup> and so on.

In this Communication, we present a new strategy to fabricate surface nanotemplates featuring well-ordered nanocavity arrays made up by C<sub>60</sub> molecules, referred to as a C<sub>60</sub> nanomesh, which is formed by precisely adjusting the binary molecular phases of C<sub>60</sub> and pentacene on Ag(111). It is demonstrated that this C<sub>60</sub> nanomesh can act as an effective template for the selective inclusion of guest C<sub>60</sub> into the nanocavities, giving rise to the formation of ordered 2D C<sub>60</sub> arrays with large intermolecular distance (2.10 nm) between the nearest neighbor C<sub>60</sub> molecules atop the C<sub>60</sub> nanomesh template.

The experiments were carried out in a multichamber ultrahigh vacuum (UHV) system housing an Omicron low-temperature scanning tunneling microscope (LT-STM) with a base pressure better than  $6 \times 10^{-11}$  mbar. The STM is interfaced to a Nanonis controller (Nanonis, Switzerland). A single-crystal Ag(111) substrate was cleaned by repeated cycles of Ar<sup>+</sup> sputtering and subsequent annealing to 800 K. The pentacene and C<sub>60</sub> molecules were thermally evaporated from separate Knudsen cells, respectively, in the UHV growth chamber (base pressure better than  $3 \times 10^{-10}$  mbar). The deposition rates for pentacene and C<sub>60</sub> were 0.2 ML/min and 0.05 ML/min, respectively, calibrated by a quartz microbalance (QCM) and STM (1 ML corresponds to a close-packed molecular layer). STM images were acquired in constant-current mode with a chemically etched tungsten tip at 77 K.

As shown in Figure 1a, a highly ordered pentacene molecular array is formed after depositing 0.7 ML pentacene on Ag(111) held

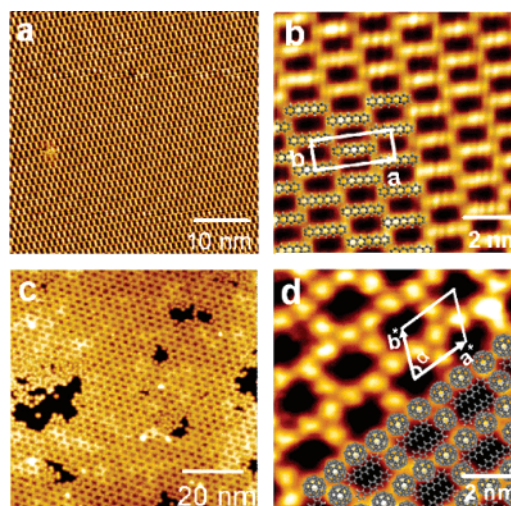


**Figure 1.** (a) STM image of long-range ordered pentacene superstructures on Ag(111). (b) Corresponding molecular resolution image ( $V_T = -1.50$  V,  $I_t = 85$  pA) of the pentacene superstructure. A unit cell is outlined on the image. (c) Large scale STM image of 0.7 ML C<sub>60</sub> self-assembled into a 2D nanomesh on pentacene ( $V_T = 2.41$  V,  $I_t = 80$  pA). (d) Detailed image of C<sub>60</sub> nanomesh; a proposed model is superimposed on the image ( $V_T = -1.49$  V,  $I_t = 100$  pA).

at room temperature and subsequently annealed to 380 K. In the corresponding high-resolution STM image (Figure 1b), the rod-like feature represents a single pentacene molecule. On Ag(111), pentacene molecules orient with their  $\pi$ -plane parallel to the substrate surface as a result of the strong interfacial interaction between the  $\pi$  electrons in pentacene and metal d-bands in Ag(111).<sup>14</sup> The periodicity perpendicular to the pentacene rows is 1.45 nm. In contrast to the typical close packed structure of monolayer pentacene on other substrates,<sup>15</sup> pentacene on Ag(111) adopts a loosely packed structure with a wide intermolecular distance of 1.03 nm along the molecular rows. As shown in Figure 1b, the voids between the pentacene molecules form a loose brick-wall-like structure as illustrated by the schematic model superimposed on the image. The white rectangle in Figure 1b highlights the unit cell ( $a = 2.90$  nm,  $b = 1.03$  nm) of the loosely packed pentacene on Ag(111).

Depositing of 0.7 ML C<sub>60</sub> onto this pentacene superstructure at room temperature and subsequently annealing to 360 K gave rise to the formation of an extended 2D network with well-ordered nanocavities (Figure 1c). The high-resolution STM in Figure 1d reveals that the nanocavity array is constituted by a regular arrangement of C<sub>60</sub> molecular chains with 1.82 nm interchain spacing, interlinked by individual C<sub>60</sub> molecules with periodicity of 2.62 nm along the chain direction, and is therefore referred to as the C<sub>60</sub> nanomesh. A unit cell of the regular nanomesh is highlighted with  $\mathbf{a}^* = 2.62$  nm,  $\mathbf{b}^* = 2.10$  nm, and  $\alpha = 60^\circ$ . The intermolecular distance between nearest neighbor C<sub>60</sub> molecules in the nanomesh is measured to be 1.05 nm, close to the van der

<sup>†</sup> Department of Physics.

<sup>‡</sup> Nanoscience and Nanotechnology Initiative.

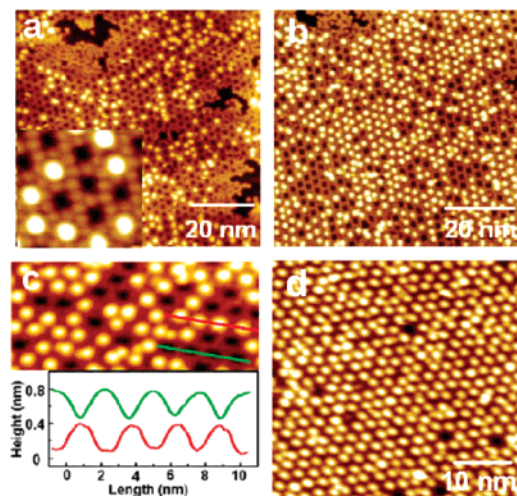


**Figure 2.** STM images of the coverage dependent evolution of  $C_{60}$  assembled on the  $C_{60}$  nanomesh ( $V_T = -2.52$  V,  $I_t = 80$  pA): (a) 0.05 ML, (b) 0.2 ML, (c) cross-sectional profiles of  $C_{60}$  assemblies (red) and nanomesh (green) as marked in the image. (d) At higher coverages (0.4 ML), the majority of the cavity sites are occupied by guest molecules and an ordered 2D  $C_{60}$  molecular array forms.

Waals distance of 1 nm in  $C_{60}$  solids.<sup>16</sup> It was known that in binary molecular systems, such as  $C_{60}$  with porphyrins,<sup>17</sup>  $C_{60}$  with acridine-9-carboxylic acid,<sup>18</sup> and tunable  $C_{60}$  linear chain arrays with  $\alpha$ -sexithiophene,<sup>19</sup>  $C_{60}$  molecules could induce a local rearrangement or conformational change of the predeposited molecule layers, which in turn influences the assembly of regular  $C_{60}$  molecular arrays. In our experiments, STM observations at defect sites of the nanomesh reveal that the arrangement of the pentacene superstructure was significantly modified by the inclusion of  $C_{60}$ . As such, a tentative model superimposed in Figure 1d is proposed for the formation of nanomesh. It involves the  $C_{60}$  adsorption induced structural rearrangement of pentacene into pentacene pair arrays, accompanied by the decoration of  $C_{60}$  aside the pentacene pairs and thereby the formation of the  $C_{60}$  nanomesh.

$C_{60}$  molecules were then evaporated onto the  $C_{60}$  nanomesh at room temperature to evaluate its effectiveness in accommodating guest molecules in the nanocavities. As shown in Figure 2a, after depositing 0.05 ML  $C_{60}$  on the nanomesh, isolated  $C_{60}$  molecules randomly distribute over the surface. In addition, short  $C_{60}$  molecular chains mostly composed of three or four  $C_{60}$  molecules can also be seen following the directions of the skeleton provided the nanomesh. A corresponding high-resolution image is shown in the inset in Figure 2a, which clearly reveals that  $C_{60}$  molecules exclusively adsorb in the nanocavities of the nanomesh template. Upon increasing the  $C_{60}$  coverage to 0.2 ML (Figure 2b), nearly half of the nanocavities are occupied by  $C_{60}$ . Notably, longer  $C_{60}$  molecular chains composed of tens of  $C_{60}$  molecules were observed at this stage. Figure 2c (bottom) presents the line profiles of a  $C_{60}$  molecular chain (red) and the underlying nanocavity array (green), as indicated in the corresponding STM image (upper panel). Obviously, the periodicity (2.62 nm) along the  $C_{60}$  chain direction matches that of the underlying nanocavity array in the same direction, indicating that the  $C_{60}$  assembly sites correspond to the topography of the  $C_{60}$  nanomesh.<sup>6,8,9,13</sup> It also confirms the trapping of  $C_{60}$  molecules in the nanocavities of the nanomesh template. Upon further increasing the  $C_{60}$  coverage to 0.4 ML (Figure 2d),  $C_{60}$  molecules almost completely occupy the nanocavities of the nanomesh template, forming an ordered 2D  $C_{60}$  molecular array. We propose that the topographic features of the  $C_{60}$  nanomesh can

immobilize individual  $C_{60}$  within the nanocavities and therefore drive  $C_{60}$  to assemble into the ordered 2D molecular array.

In summary, an extended 2D  $C_{60}$  nanomesh has been constructed by controlling the binary molecular phases of  $C_{60}$  and pentacene on Ag(111). The skeleton of the  $C_{60}$  nanomesh is stabilized by the strong molecule–metal interfacial interactions [ $C_{60}$ –Ag(111) and pentacene–Ag(111)] and is further modified by the pentacene– $C_{60}$  donor–acceptor intermolecular interactions. This  $C_{60}$  nanomesh can serve as an effective template to selectively accommodate guest  $C_{60}$  molecules at the nanocavities, thereby leading to the formation of an ordered 2D  $C_{60}$  array with a large intermolecular distance (2.10 nm) between the nearest neighboring  $C_{60}$  on top of the  $C_{60}$  nanomesh template.

**Acknowledgment.** W.C. acknowledges financial support by a LKY PDF fellowship. The authors acknowledge support from A\*STAR grant R-398-000-036-305 and ARF grant R-144-000-196-112.

## References

- (1) (a) Joachim, C.; Ratner, M. A. *Proc. Natl. Acad. Sci. U.S.A.* **2005**, *102*, 8801. (b) Joachim, C.; Gimzewski, J. K.; Aviram, A. *Nature* **2000**, *408*, 541. (c) Selzer, Y.; Allara, D. L. *Annu. Rev. Phys. Chem.* **2006**, *57*, 593. (d) Nitzan, A.; Ratner, M. A. *Science* **2003**, *300*, 1384. (e) Carroll, R. L.; Gorman, C. B. *Angew. Chem. Int. Ed.* **2002**, *41*, 4378.
- (2) (a) Burkard, G.; Loss, D.; DiVincenzo, D. P. *Phys. Rev. B* **1999**, *59*, 2070. (b) Benjamin, S. C.; Ardavan, A.; Briggs, G. A. D.; Britz, D. A.; Gunlycke, D.; Jefferson, J.; Jones, M. A. G.; Leigh, D. F.; Lovett, B. W.; Khllobystov, A. N.; Lyon, S. A.; Morton, J. J. L.; Porfyrakis, K.; Sambrook, M. R.; Tyrushkin, A. M. *J. Phys.: Condens. Matter* **2006**, *18*, S867.
- (3) (a) Blawas, A. S.; Reichert, W. M. *Biomaterials* **1998**, *19*, 595. (b) Rosi, N. L.; Mirkin, C. A. *Chem. Rev.* **2005**, *105*, 1547. (c) Park, T. J.; Lee, S. Y.; Lee, S. J.; Park, J. P.; Yang, K. S.; Lee, K.-B.; Ko, S.; Park, J. B.; Kim, T.; Kim, S. K.; Shin, Y. B.; Chung, B. H.; Ku, S.-J.; Kim, D. H.; Choi, I. S. *Anal. Chem.* **2006**, *78*, 7197.
- (4) (a) Barth, J. V.; Costantini, G.; Kern, K. *Nature* **2005**, *437*, 671. (b) Chen, W.; Wee, A. T. S. *J. Phys. D: Appl. Phys.* **2007**, *40*, 6287. (c) Rosei, F. *J. Phys.: Condens. Matter* **2004**, *16*, S1373.
- (5) (a) Chen, W.; Xu, H.; Liu, L.; Gao, X. Y.; Qi, D. C.; Peng, G. W.; Tan, S. C.; Feng, Y. P.; Loh, K. P.; Wee, A. T. S. *Surf. Sci.* **2005**, *596*, 176. (b) Chen, W.; Loh, K. P.; Xu, H.; Wee, A. T. S. *Langmuir* **2004**, *20*, 10779.
- (6) Corso, M.; Auwärter, W.; Muntwiler, M.; Tamai, A.; Greber, T.; Osterwalder, J. *Science* **2004**, *303*, 217.
- (7) Deak, D. S.; Sully, F.; Porfyrakis, K.; Castell, M. R. *J. Am. Chem. Soc.* **2006**, *128*, 13976.
- (8) (a) Theobald, J. A.; Oxtoby, N. S.; Phillips, M. A.; Champness, N. R.; Beton, P. H. *Nature* **2003**, *424*, 1029. (b) Staniec, P. A.; Perdigão, L. M. A.; Saywell, A.; Champness, N. R.; Beton, P. H. *Chem. Phys. Chem.* **2007**, *8*, 2177.
- (9) Spillmann, H.; Kiebele, A.; Stöhr, M.; Thomas, A. J.; Bonifazi, D.; Cheng, F. Y.; Diederich, F. *Adv. Mater.* **2006**, *18*, 275.
- (10) Pan, G. B.; Liu, J. M.; Zhang, H. M.; Wan, L. J.; Zheng, Q. Y.; Bai, C. L. *Angew. Chem., Int. Ed.* **2003**, *42*, 2747.
- (11) Lu, J.; Lei, S.; B.; Zeng, Q. D.; Kang, S. Z.; Wang, C.; Wan, L. J.; Bai, C. L. *J. Phys. Chem. B* **2004**, *108*, 5161.
- (12) Dmitriev, A.; Spillmann, H.; Lin, N.; Barth, J. V.; Kern, K. *Angew. Chem., Int. Ed.* **2003**, *42*, 2670.
- (13) (a) Stepanow, S.; Lingenfelder, M.; Dmitriev, A.; Spillmann, H.; Delvigne, E.; Deng, X.; Cai, C.; Barth, J. V.; Kern, K. *Nat. Mater.* **2004**, *3*, 229. (b) Stepanow, S.; Lin, N.; Barth, J. V.; Kern, K. *Chem. Commun.* **2006**, 2153.
- (14) (a) Thayer, G. E.; Sadowski, J. T.; zu Heringdorf, F. M.; Sakurai, T.; Tromp, R. M. *Phys. Rev. Lett.* **2005**, *95*, 256106. (b) Chen, W.; Wang, L.; Qi, D. C.; Chen, S.; Gao, X. Y.; Wee, A. T. S. *Appl. Phys. Lett.* **2006**, *88*, 184102.
- (15) (a) Guaino, Ph.; Cafolla, A. A.; Carty, D.; Sheeran, G.; Hughes, G. *Surf. Sci.* **2003**, *540*, 107. (b) Schroeder, P. G.; France, C. B.; Park, J. B.; Parkinson, B. A. *J. Appl. Phys.* **2002**, *91*, 3010. (c) France, C. B.; Schroeder, P. G.; Forsythe, J. C.; Parkinson, B. A. *Langmuir* **2003**, *19*, 1274.
- (16) Heiney, P. A.; Fischer, J. E.; McGhie, A. R.; Romanow, W. J.; Denenstien, A. M.; McCauley, J. P.; Smith, A. B.; Cox, D. E. *Phys. Rev. Lett.* **1991**, *66*, 2911.
- (17) Bonifazi, D.; Spillmann, H.; de Wild, M.; Seiler, P.; Cheng, F. Y.; Guentherodt, H. J.; Jung, Thomas, A.; Diederich, F. *Angew. Chem., Int. Ed.* **2004**, *43*, 4759.
- (18) Xu, B.; Tao, C. G.; Williams, E. D.; Reutt-Robey, J. E. *J. Am. Chem. Soc.* **2006**, *128*, 8493.
- (19) (a) Zhang H. L.; Chen W.; Chen L.; Huang H.; Wang X. S.; Yuhara J.; Wee A. T. S. *Small* **2007**, *3*, 2015. (b) Chen L.; Chen W.; Huang H.; Zhang H. L.; Yuhara J.; Wee A. T. S. *Adv. Mater.* In press.

JA710009Q